Final report

1.1   Project details

Project title	A Live PV Testing Platform for Larger Adoption – PVTP
Project identification (program abbrev. and file)	Energinet.dk ForskEL project no. 12421
Name of the programme which has funded the project	ForskEL
Project managing company/institution (name and address)	Technical University of Denmark Elektrovej building 325, Center for Electric Power and Energy Kgs. Lyngby 2800
Project partners	Bornholms Energy og Forsyning Kenergy Eniig Solarconnectivity
CVR (central business register)	30060946
Date for submission	31 Dec 2018

1.2   Short description of project objective and results

The project aims to develop a testing platform for solar PV plants for testing and verifying their grid support functions. The platform is located in the actual grid of Bornholm. The latest communication protocol SunSpec for communication with solar PV inverters is implemented in the remote terminal units of the grid operator's SCADA so the plant becomes an integral part of the grid control system. The PV plant functions are first verified in a lab environment before being implemented in the actual system. The platform is successfully delivered in the project. The results and learnings can accelerate the applications of the functionalities embedded in modern solar PV plants for grid support and eventually contribute to the uptake of solar energy in the distribution grids.

Projektets formål er at udvikle en testplatform for solcelleanlæg til at teste og efterprøve deres systemydelser til nettet. Platformen er opbygget i forsyningsnettet hos Bornholms Energi og Forsyning. Den nyeste kommunikationsprotokol SunSpec til kommunikation med solcelleanlægs inverterer, er implementeret i en decentral kommunikationsenhed (RTU) i netoperatørens SCADA system, således at solcelleanlægget er blevet en integreret del af netstyringssystemet. Funktionaliteten blev først verificeret i laboratoriet, før det blev implementeret i det eksisterende system. Det samlede system er fuldt kørende ved projektets afslutning og fungerer tilfredsstillende. Resultaterne og læringen kan fremskynde anvendelsen af funktionaliteter som er indbyggede i moderne solcelleinvertere til at levere systemydelser og evt. bidrage til at øge absorbering af solenergi i lavspændingsnettet.

1.3   Executive summary

The project delivered a test platform in the grid of Bornholm and verified the grid support functions of solar PV inverters. The project is the first one that integrates the control functions of solar PV inverters as part of the SCADA system of distribution grid in Denmark. A 176.8-kW solar PV plant located in the grid of Bornholm is used as the targeted site. The communication link between the solar PV inverters and the remote terminal unit (RTU) is established through implementing the SunSpec protocol[1,2] in the RTU, which is the key to enable the remote access of the measurements and control settings of inverters from the control room of the distribution

---

[1] SunSpec Alliance, "SunSpec Alliance: Information Standards for Distributed Energy," www.sunspec.org

[2] Sunspec is required by ENDK TF3.2.2, cf. section 7.3.

grid. By the test platform, the essential monitoring and control functions of PV plants for grid support in normal operation are tested and effects are verified in the field.
NB: Sunspec is required by TR3.2.2, cf. 7.3.

The project also developed a laboratory testbench to cover additional tests on the inverter control functions during the grid dynamics. Additional tests, such as frequency support, fault ride through, and unbalanced operation of inverters, are implemented via a 150-kVA 4-quadrant grid-forming power amplifier connected with the inverter. A testing program is developed in NI CompactRIO (NI cRIO) device which can generate variable and controllable voltage signals as input to the power amplifier. The power amplifier amplifies the modulated voltage signal and presents it to the inverter. All voltages and currents at the terminal of the inverter are measured and recorded by meters with the high sampling frequency.

The project also developed system level studies on the value of the reactive power from solar PV plants to the grid operator. The medium voltage grid of the entire Bornholm system is studied under different penetration levels of solar PV systems and reactive power control functions. The study will help the grid operators to develop control strategies on the reactive power support from solar PV inverters for grid support.

1.4 Project objectives

Reliable solar photovoltaic (PV) generation technology has high potential to contribute significant electric energy to society. Thanks to modern power electronic technology, solar PV plants provide many opportunities to support the grid operation, automatically or by command. However, grid operators nowadays are still reluctant to welcome more PV installations to their grids.

The reason behind lies in the fact that most of the solar PV plants are relatively small in size compared with conventional power plants or many other types of renewable energy sources, and they are usually installed in the deep of the electric network, e.g. in the 0.4-kV low voltage network, which makes their controllability and benefits hard to be seen and utilised by the system operators. This makes difficulties for the operators to accommodate PV plants in operation and planning.

Given the ever-decreasing cost of PV systems, Denmark will likely keep up with the trend. Currently, grid operators, both at transmission and distribution levels, have seen opportunities for utilising PV systems to solve different kinds of grid issues [1]. There have been many projects funded both for increasing the PV penetration level, as well as utilising PV control to aid operators [2].

However, there is still reluctance from utilities worldwide to have large amounts of PV energy in their grids, letting alone exploit the advances of PV systems for grid operational security. This is due to the fact that most PV systems have relatively smaller sizes than other power plants and their control systems are running spontaneously within the system, the functionalities of PV inverters, though many are required by the grid operators, are still considered "nice to have," instead of "essential to have." There is still a barrier between technology and practice. Given the facts above, the aim of the project is hereby formulated below to break the barrier between technology and real-world practice.

Develop a live PV laboratory for testing, research and education.

Above overall objective is incorporated with a few technical objectives that will be achieved in the first place:

- Able to test the control capabilities of PV plants for supplying ancillary services for normal system operation;
- Able to test PV inverter inertia contribution, short-circuit power contribution and power quality.
- Able to test more advanced frequency and reactive power control strategies

- Utilising the communication capabilities of the latest inverters to achieve scalable and reliable operation.
- The PV systems are well monitored with the measurements archived. This enables further data analysis can be used for both research and education.

1.5 Project results and dissemination of results

The results of the project are organized according to three sections reflecting the work arrangement of technical work packages.

1.5.1 Integration of solar PV plants in the grid operator's SCADA

In this part, the main target is to implement an open protocol from SunSpec Alliance [3] in the industrial standard remote terminal unit (RTU), used by the distribution grid SCADA system, to achieve the communication between RTU and PV inverters. The SunSpec Alliance is a trade alliance composing more than 100 solar, storage and distributed energy industrial partners, in order to pursue a common information model that can enable "plug & play" at the distribution system for interoperability. They have now already been accepted by many solar inverter manufacturers.
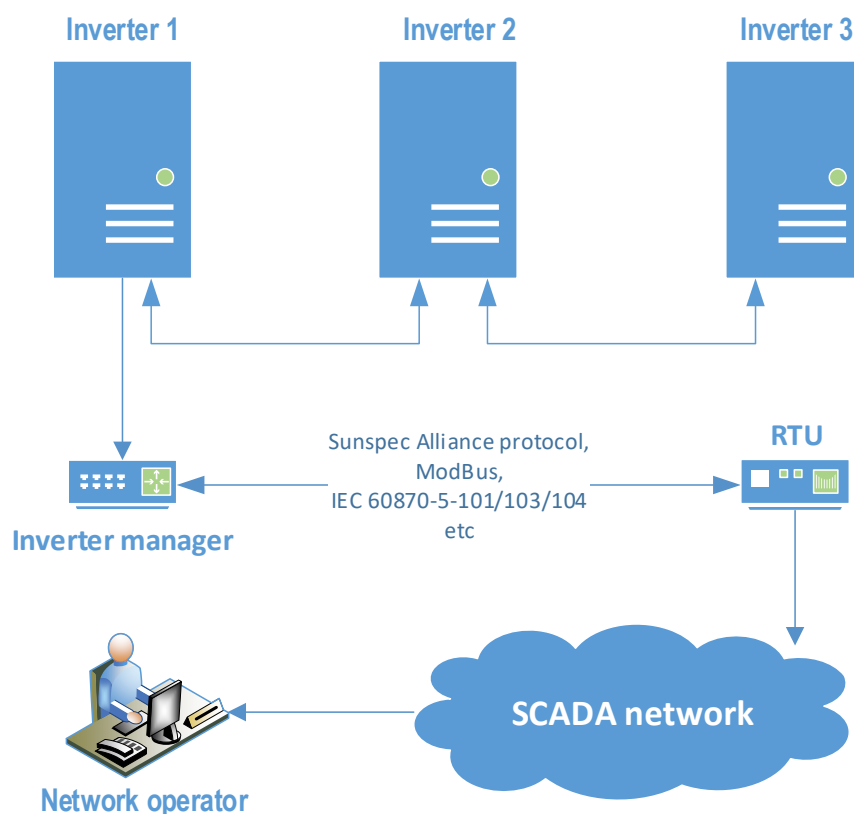

Figure 1.5-1 Structure of the communication system

By this means, the distribution grid operator on Bornholm (Bornholms Energi og Forsyning, BEOF) in the control room can remotely poll the inverter measurements and send control signals to regulate the output when there is a necessity. The structure of the discussed communication system is illustrated in Figure 1.5-1. The control of the inverters is realised by an inverter manager which communicates with all the PV plants consisting of three inverters. The RTU is programmed so that it is able to communicate with the inverters, and the SCADA system is also updated in order to enable the integration of the RTU. With this proposed system, the grid operator in the control room is able to monitor and control the inverters remotely. The communication between the inverter manager and the RTU is realized via the SunSpec Alliance protocol.

Before going to the field, the protocol is tested in the laboratory on a single-phase inverter, which is compatible with the SunSpec protocol. The inverter used in the test is powered by a programmable DC power supply and connected to the laboratory grid and its output is

measured by the laboratory SCADA system. The RTU is programmed for SunSpec protocol and connected to the inverter. Then the information received by the RTU is compared with the data acquired by the SCADA system so that the accuracy of the received information can get verified and validated. The test reports for the verification on the measurements and the setpoints are given in Table 1.5-1 and 1.5-2, respectively. The SCADA measurements have opposite signs in power and power factor because of the selected reference direction. From Table 1.5-1 and 1.5-2, it can be seen that the values communicated through the SunSpec protocol reach a good agreement with the SCADA and the inverter measurements.

Table 1.5-1 Verification on the measurements

Signal	Unit	RTU	SCADA	Inverter
Freq	Hz	50.05		50.05
PF	*cosφ*	1	1	
V_a	Volt	238.1	237	
S	VA	1400		
P	W	1410	-1380	1415
Q	var	0	0	0

Table 1.5-2 Verification on the setpoints

Signal	Unit	RTU	SCADA	Inverter
P_{set}=50%	W	750	-680	750
P_{set}=0%	W	10	0	10
Q_{set}=-60%	var	-760	760	
Q_{set}=60%	var	750	-700	
PF=0.8	*cosφ*	-0.8	0.81	
PF=-0.8	*cosφ*	0.799	-0.78	

The validation communication process between the RTU and the inverter manager located at Campus Bornholm is conducted, as shown in Figure 1.5-2. The measurements that can be polled from the inverter includes per phase voltage, active and reactive power, power factor, and frequency, while the parameters that can be set include the maximum percentage of active power, the setpoint of reactive power and the power factor.
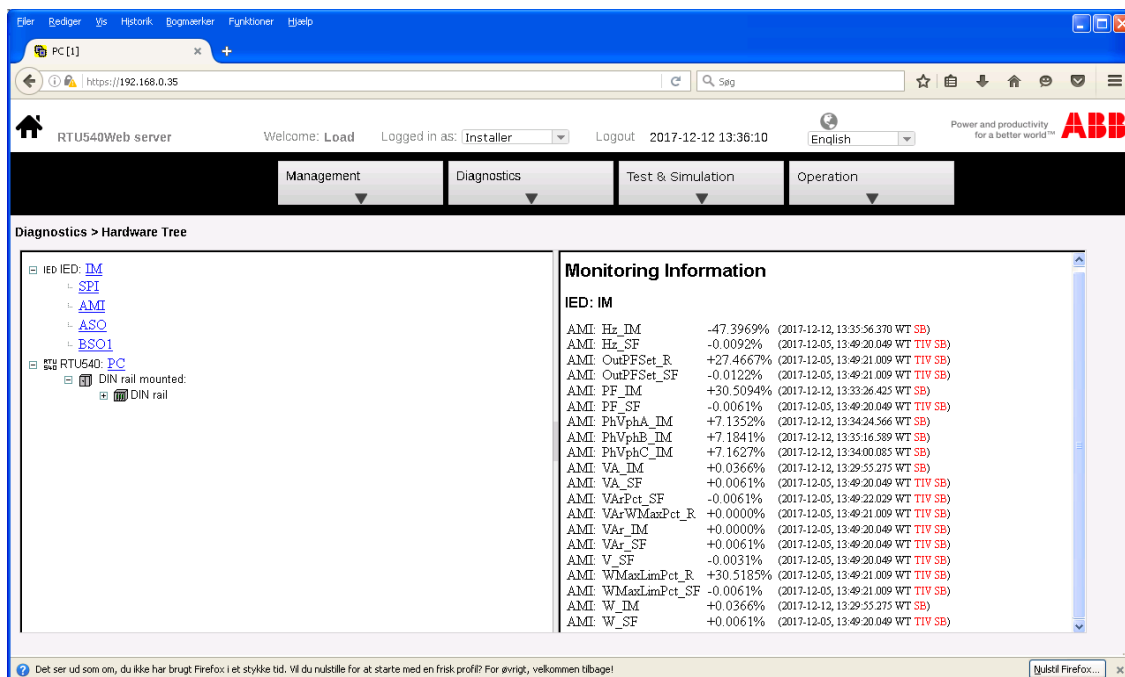

Figure 1.5-2 Validation of the communication

After the communication protocol of SunSpec is implemented, the SCADA system in the control room of the system operator (BEOF) is updated so that the measurement points are integrated into the SCADA system with the user interface update that enables the operator to monitor and control the Campus' solar power plant.

The photos below present the installation of the RTU and the measurement equipment at Campus and the 10/0.4 kV transformer station at Campus (Bornholm).

Photo 1. Setup of the RTU and measurement system at campus

Photo 2. Setup of the RTU and measurement system in the 10/0.4-kV transformer station supplying the campus

Consequently, BEOF is now able to regulate the active and reactive power on the plant and therefore regulate the system in relation to the current network conditions. It must be possible to provide reactive power at night (Q@night function) as well when there is no active power from the PV power plants, because the inverters are usually set in sleep mode for the purpose of energy saving during the night, in which way the electricity company can regulate the reactive power independent of time. In this case, the reactive power function of the inverter is as effective as a distribution system STATCOM. The entire structure of the proposed implementation is illustrated in Figure 1.5-3.
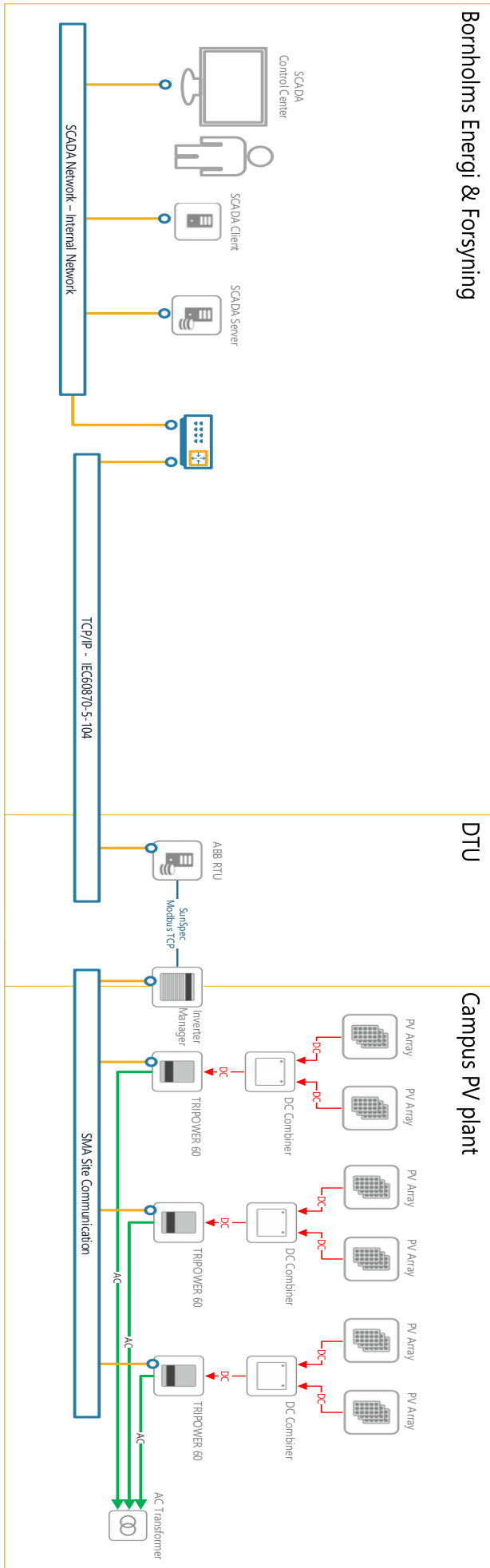
Figure 1.5-3 Structure of the entire system

Furthermore, it is necessary to investigate the effect of regulation of the plant on the local network and how it should thus be regulated in relation to it. In addition, it should be clarified whether the operation and regulation of the plant have an effect on the life of inverters, transformers and cables. In practice, BEOF changed the 10/0.4 kV transformer where the solar PV plant connected to and has installed an RTU, particularly for the transformer to collect data of the transformer temperature, currents and voltages so that the reliability of the services from the solar PV plant can get verified.

1.5.2 Laboratory testing platform development

In this part, the main task is to develop a platform in the laboratory for testing the performance of PV inverters under unbalanced operation and fault conditions. The platform is established based on the facility provided by PowerLabDK located at DTU Lyngby Campus. The layout of the developed platform in the laboratory is shown in Figure 1.5-4.
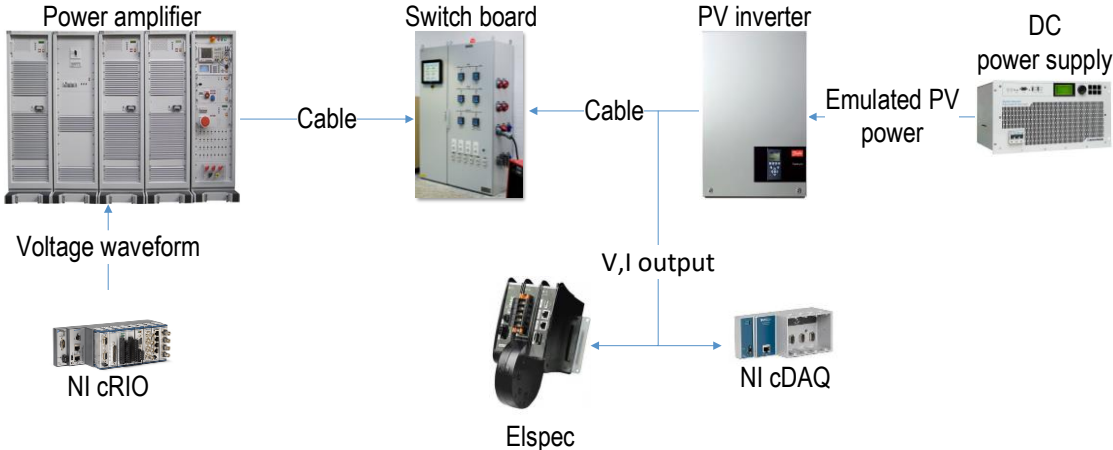

Figure 1.5-4 Test platform in the laboratory

At the inverter side, a programmable DC power supply is adopted instead of real PV modules providing emulated PV power because real PV generation is highly dependent on solar irradiance and ambient temperature. In this way, the intermittent nature of solar power is therefore eliminated. At the power amplifier side, an NI cRIO device works as a voltage waveform generator supplying a fully controllable three-phase voltage to the power amplifier, forming a simulated low-voltage power grid. The test results are acquired by Elspec, a power quality analyzer with high sampling rate, and an NI CompactDAQ (NI cDAQ) device. These two sides are connected through the switchboard called LabCell.

The inverter used in this experiment is a three-phase inverter manufactured by Danfoss with a full capacity of 10 kW (Type TLX 10+ Pro) and the power amplifiers used in the experiment have a capacity of 150 kVA, manufactured by Spitzenberger. The amplifiers have a fairly short response time under dynamic processes, in the dimension of a microsecond.

Based on this laboratory platform, the performance of PV inverter is tested under different unbalanced conditions, i.e. single- and double-phase imbalance, and fault conditions, including balanced fault, single- and double-phase fault. All the configurations on the parameters during the tests follow the requirements in the Danish grid code for power plants up to and including 11 kW, namely Teknisk Foreskrift 3.2.1 (TF 3.2.1) [4].

The control of the input voltage waveform, including frequency, RMS value, phase angle and fault condition, is realised by means of the human-machine interface (HMI) built in NI LabVIEW illustrated in Figure 1.5-5. In this way, the amplifier works as a controllable simulated low-voltage power grid. By changing the value in "Voltage ratio" and clicking the buttons in "Voltage control panel", different types and severities of unbalanced operation, as well as different types of fault conditions, can be implemented to the simulated power grid.
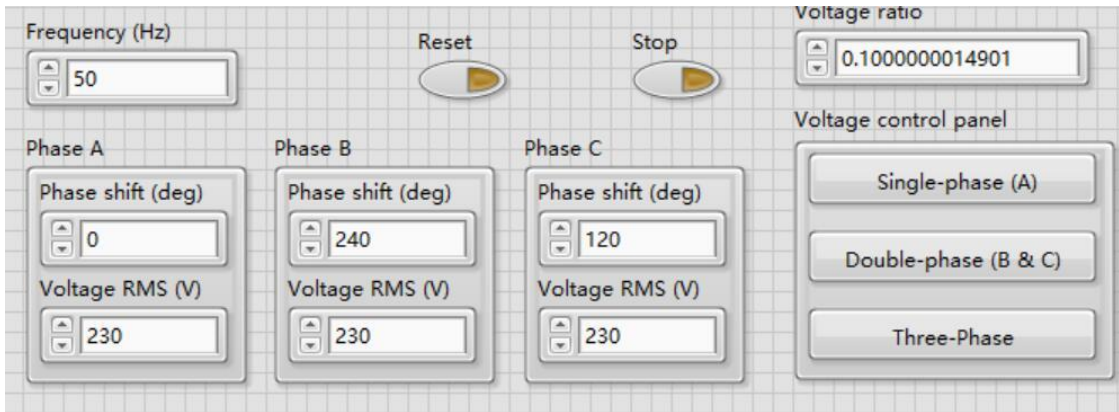
Figure 1.5-5 HMI in LabVIEW

The unbalanced conditions are tested with the full capacity of the inverter, i.e. 10 kW. Two different dynamic reactive power support functions, including the dynamic power factor support (*PF*(*P*) control) and the dynamic reactive power support (*Q*(*V*) control), and the primary frequency response function, are investigated under two unbalanced conditions, i.e. single- and double-phase unbalanced operation. To compare the effects from unbalanced conditions clearly and intuitively, a benchmark is also made by performing a balanced three-phase test with a voltage of all three phases ranging from 0.93 p.u. to 1.09 p.u. Likewise, in the unbalanced condition tests, the voltage at the corresponding unbalanced phase(s) alters within the same range. In terms of the frequency response test, the voltage magnitude of the unbalanced phase(s) is controlled at 0.95 p.u. and 1.05 p.u., respectively. In the single-phase unbalanced case, only the voltage of Phase A changes while the voltage of Phase B and C changes in the double-phase unbalanced case. In the benchmark case, the voltage of all three phases changes simultaneously.

Different fault conditions, including balanced, single- and double-phase fault, are realised by instantly reducing the voltage magnitude of the corresponding phase(s) to an extremely low value, 0.1 per unit in this project. The fault condition tests are conducted under 5 different active power output levels, including 1.5 kW, 3 kW, 5 kW, 7 kW and the rated output, 10 kW. Different output levels can be adjusted by changing the configuration of the programmable DC power supply. In the tests, the fault current (I_{SC}) contribution and the disconnection time are investigated and compared.

With the tests described in the previous paragraphs, the performance of the PV inverter is analysed by considering the phase and sequence components of voltage and current, and active and reactive power output from the inverter.

From the unbalanced operation tests, it is found that the output current is controlled to maintain the active power output during the change of voltage magnitude as expected. Furthermore, the inverter can provide the grid with reactive power support by injecting reactive power to the grid when the voltage magnitude is below 1 p.u. and absorbing when the voltage magnitude is above 1 p.u.

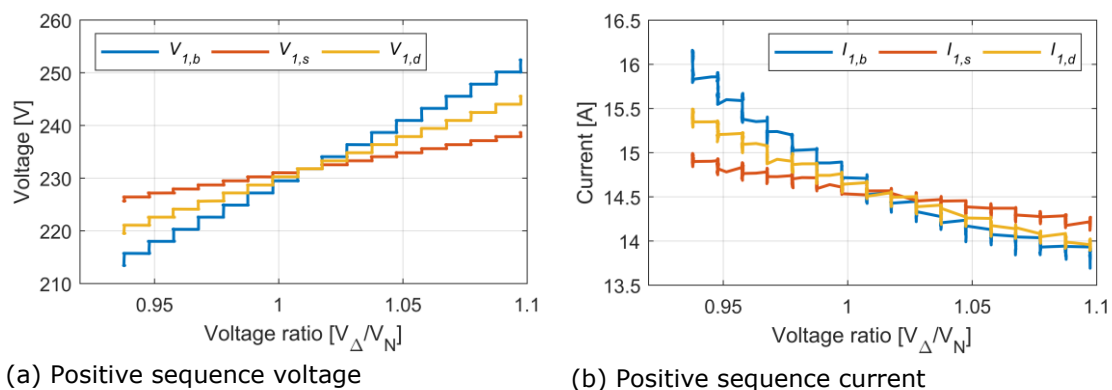(a) Positive sequence voltage

(b) Positive sequence current

Figure 1.5-6 Positive voltage and current under balanced, single- and double-phase unbalanced operation

By comparing all the three scenarios under the $Q(V)$ control, the relation between positive sequence voltage V_1 and current I_1 is revealed. In Figure 1.5-6a and b, the x-axis represents the ratio between the voltage in the specific unbalanced case V_Δ and the nominal voltage V_N, and the balanced, single- and double-phase unbalanced condition are represented by subscripts b, s and d respectively. Besides, the voltage at the terminal is slightly higher than the voltage input by the cRIO, which is partly caused by the small fluctuation and oscillation in the amplifier output, as well as the active power output from the inverter, which can cause voltage rise.

Furthermore, it can be observed from Figure 1.5-6a that regardless the operation condition, there is a linear relation between V_1 and the ratio of V_Δ and V_N, while a reverse relation between I_1 and the ratio of V_Δ and V_N can be seen from Figure 1.5-6b, which potentially maintains the nearly constant active power output.
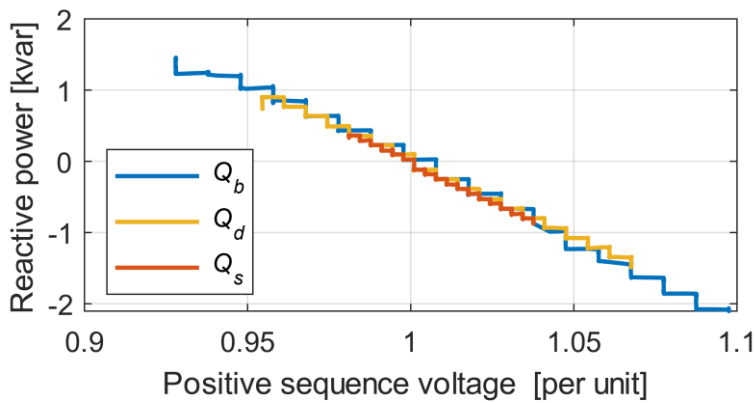

Figure 1.5-7 Reactive power response under balanced, single- and double-phase unbalanced operation

As shown in Figure 1.5-7, the reactive power output from the inverter under three scenarios with $Q(V)$ control applied is compared. With the x-axis representing V1 plotted in Figure 1.5-3, it is verified that the reactive power output is directly controlled by the positive sequence voltage. The amount of the reactive power under unbalanced operation is proportional to that under balanced condition. The amount of Q_b is three times the amount of Q_s and 1.5 time the amount of Q_d.

In the below-nominal zone (under-voltage situation, magnitude lower than 1 p.u.), the inverter provides voltage regulation by injecting inductive reactive power while the inverter absorbs reactive power or injects capacitive reactive power to regulate the voltage in the above-nominal zone (over-voltage, magnitude higher than 1 p.u.), represented by minus output. Furthermore, it can also be seen that from balanced to double-phase unbalanced, then to the single-phase case, the range of V1 becomes narrower and narrower and the available reactive power support is smaller and smaller at the same time.

(a) Balanced operation
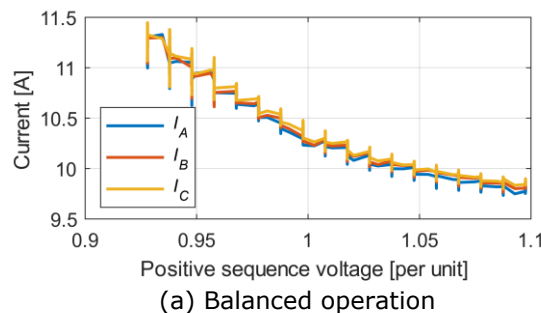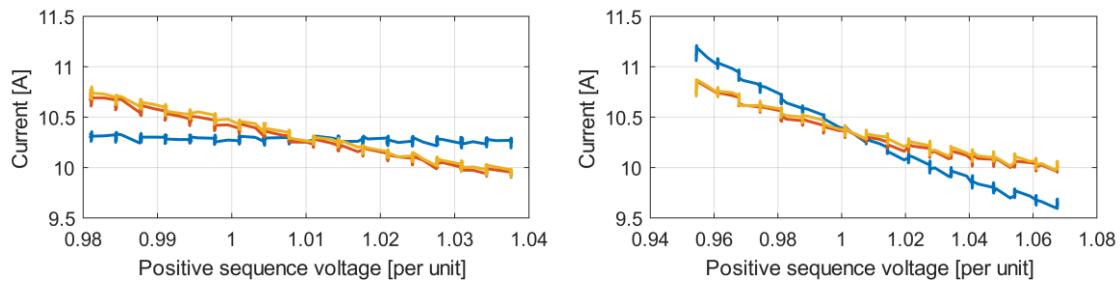
(b) Single-phase unbalanced operation   (c) Double-phase unbalanced operation

Figure 1.5-8 RMS current under balanced, single- and double-phase unbalanced operation

The root-mean-square (RMS) current of each phase under all three scenarios are plotted in Figure 1.5-8a to c. From Figure 1.5-8a, it is clearly seen that the current of all three phases drops in the same trend as the positive sequence voltage increases under balanced operation. Under unbalanced cooperation, however, the current of balanced phase(s) drops faster than the unbalanced phase(s), which is especially obvious in the single-phase case. It is verified that the output current of PV inverter is directly controlled by the positive sequence voltage. From Figure 1.5-8b and c, it can be observed that the largest current difference between phases is within 0.5 A, which complies with the requirement in TF 3.2.1.

Because the change in the current of each phase, the active power of the balanced phase(s) decreases while that of the unbalanced phase(s) increases, which consequently maintains the total active power output at an approximately constant level as the voltage unbalanced severity varies.
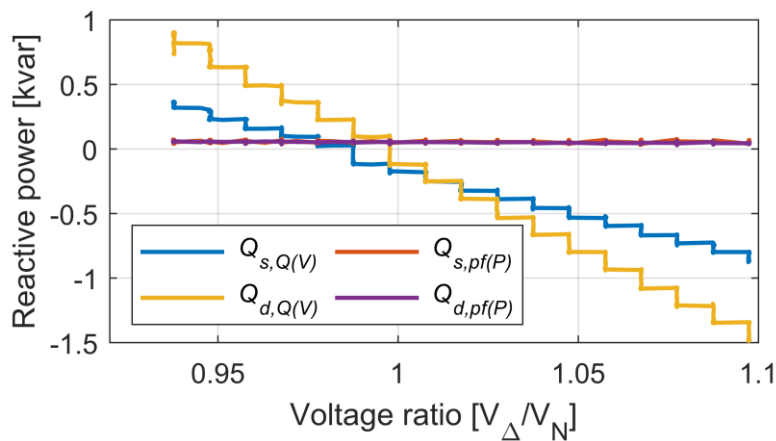

Figure 1.5-9 Comparison between $Q(V)$ and $PF(P)$ control under balanced, single- and double-phase unbalanced operation

A comparison between $Q(V)$ and $PF(P)$ control is conducted under single- and double-phase unbalanced condition and shown in Figure 1.5-6. It can be clearly seen that the total reactive power output varies as the voltage unbalanced severity changes with $Q(V)$ control implemented while it keeps constant with $PF(P)$ control applied. Since the total output active power keeps constant as stated previously, the total output reactive power is thus constant as well, as shown in Figure 1.5-9.

The test results of frequency response function are shown in Figure 1.5-10a and b, with the x-axis representing the frequency increment. In the test, the grid frequency increases from 50 Hz to 51 Hz with the activation frequency of the function being 50.4 Hz. From Figure 1.5-10a and b, it is found that the over-frequency support is not actually activated at 50.4 Hz in some conditions. In terms of the two cases conducted in this test, namely V_Δ equals 0.95 p.u. and 1.05 p.u., the actual activation frequencies of balanced, single- and double-phase scenario are 50.4 Hz, 50.4 Hz, 50.5 Hz and 50.4 Hz, 50.5 Hz, 50.5 Hz, respectively, according to the results presented in Figure 1.5-10a and b.

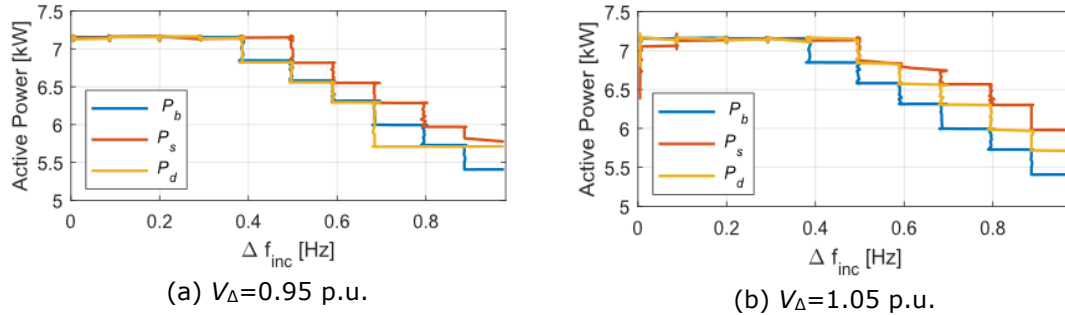(a) V_Δ=0.95 p.u.

(b) V_Δ=1.05 p.u.

Figure 1.5-10 Frequency response under balanced, single- and double-phase unbalanced operation

The results indicate that the frequency response function is affected by the unbalanced operation. One possible reason behind this is the frequency detection technique and the internal control system of the inverter. Different from conventional synchronous generators, which detect the frequency deviation based on the difference between mechanical torque and electromagnetic torque, inverter-based generation units like PV inverters utilize phase-locked loop (PLL) to capture the frequency deviation. The PLL integrated into the inverter can be either three single-phase ones or one three-phase one. The single-phase type uses positive sequence voltage extractor to acquire the positive sequence voltage of each phase and the frequency is detected at each phase separately. In this way, the inverter responses the frequency deviation based on the per phase positive sequence active power calculated with the positive sequence voltage. During an unbalanced operation, positive sequence voltage and current are lower than that in a balanced condition, as indicated in Figure 1.5-6a. Therefore, the positive sequence active power is actually lower than it should be and thereof the power reference for frequency regulation is lower which can affect adjusting active power. Thus, the imbalance in each phase may affect the performance of PLL. Another possible reason for this can be the sudden variation in the grid frequency implemented in the experiment. In the real world, sudden loss of large-scale loads, for example, can cause such sudden frequency variation, which, however, rarely happens.

The results of the fault test are summarised in Table 1.5-3, including fault current contribution represented with its peak value and the disconnection time, which is defined as the time interval between the start of the fault and the time when the inverter gets completely disconnected.

Table 1.5-3 Summary of fault condition tests

Quantity types	Fault types	Active power output [kW]				
		1.5	3	5	7	10
Peak fault current [A]	Balanced	37.16	44.43	39.27	37.84	39.03
	Single-phase	31.75	38.13	32.16	38.76	38.25
	Double-phase	30.23	34.95	36.94	36.74	37.09
Disconnection time [s]	Balanced	0.66	0.67	0.75	0.64	0.68
	Single-phase	0.71	0.61	0.79	0.64	0.86
	Double-phase	0.70	0.69	0.81	0.71	0.68

The peak values of the fault current are listed in the first three rows in Table 1.5-3. Compared with the nominal peak current of the inverter, 20.41 A, calculated with its full capacity (10 kW) and nominal voltage (0.4 kV line-to-line), the peak value of the fault current can generally reach 1.8 to 2 times the nominal value. From the perspective of the experiment results, the PV inverter can contribute considerably high fault to the grid enabling the protection scheme to detect the fault and trip protection mechanism. Additionally, it is found that the fault current is not actually affected by the actual active power output from the inverter. It is implied that the fault current contribution is determined by the full capacity of the inverter.

And the following three rows in the table list the time that takes the inverter to get disconnected from the grid during the fault process. Based on the results in Table 1.5-3, it can be seen that the disconnection time for the balanced fault is the shortest while the time for

the unbalanced fault is slightly higher. Since the fault current is the highest in a balanced fault and lowest in a double-phase fault, it is implied that the disconnection time is affected by the fault current.

1.5.3 Assessment of the value of reactive power provision from solar PV

The main target for this part is to evaluate the impacts of different reactive power support functions provided by the PV inverter from the perspective of the medium voltage (MV) grid. The assessment of reactive power support function of PV systems is conducted based on the power distribution system on Bornholm (10 kV grid).

Addition to the PV plants, there are also totally 30 MW of wind turbines installed on Bornholm currently. However, because the main target is to assess and evaluate the impacts from the PV inverters and different operating conditions of the inverters, the configuration and parameters of the wind farms and the impacts brought by them can, therefore, be treated as constants and the wind turbines are not included in the system model when the system is being evaluated.

Different reactive power support functions from the PV systems and the effects brought by increasing PV penetration level are assessed by conducting a time-series load flow calculation for one complete year with step length of one hour (365 days × 24 hours/day = 8760 hours). The power losses of the MV grid, the overloading situations of transformers and the over-voltage problems of buses are the main observations in this section. The overload state for transformers is defined as loading rate over 100% while the over-voltage states for 0.4 kV buses, 10 kV buses and 60 kV buses are defined as voltage magnitude over 1.1 p.u., 1.2 p.u. and 1.2 p.u., respectively, according to TF 3.2.1 and the grid code for PV plants above 11 kW, i.e. Teknisk Foreskrift 3.2.2 (TF 3.2.2) [4], [5]. The total power loss of the entire system is calculated by first summing up the power loss of all the system components, including transformers and cables, and then taking the average over 8760 hours.

According to the grid codes TF 3.2.1 and TF 3.2.2, PV systems should be capable of providing reactive power support to the grid and the functions include constant reactive power (constant Q) control, constant power factor (constant PF) control and the dynamic power factor support ($PF(P)$ control). The PV systems installed on Bornholm include centralised plants and small-scale residential systems. Since constant Q control is suitable for large-scale systems, it is only applied to the centralised ones.

Currently, the total installed capacity of PV systems on Bornholm is around 22 MW, including two large-scale centralised power plants of 7.5 MW and medium-scale plants of around totally 2.4 MW distributed in the 0.4 kV network. The rest are deployed as residential systems, scattered within the 0.4 kV network. In the case studies, the PVs installed in the LV grids are aggregated to the LV terminals of the 10/0.4 kV transformers. The loads are assumed to be with 0.95 of the power factor [6]. The LV grid used in this part is an LV feeder connected to a 100-kVA transformer, consisting of 32 buses connected with cables. For the purpose of clear comparison and precise observation, a base case is thereby built based on the current PV deployment, and the penetration level increases based on this base case, from the current level up to 100%.

By comparing the peak load, annual energy consumption, population and area of Bornholm and the whole of Denmark, it is concluded that the size of Bornholm is approximately 0.7% to 1.4% of the whole of Denmark. According to a previous study conducted on the optimal energy mix of wind and solar energy, a final suggested optimal combination is 80% wind energy and 20% solar energy [7], which corresponds to approximately 7000 MW of wind turbines and 7000 MW of solar PV systems. Therefore, 100 MW of total installed capacity is selected as the penetration level of 100% for the Bornholm power system, which is approximately equivalent to 1.4% of the total capacity of the whole of Denmark. Therefore, the PV penetration level in this part is defined as the ratio of the actual installation capacity of the PV systems and 100 MW. Starting from the base case, which is equivalent to a penetration level of 22% according to the definition, the assessment of different reactive power control functions is then conducted from 30% of penetration up to 100%, with an increment of 10% in between.

The first step is to set the reactive power control function to *PF*(*P*), letting the PV inverters adjust the reactive power automatically based on their active power generation. Starting from the base case (penetration level of 22%), there are totally 9 cases to be studied in this part. Based on the case study results, one specific case, together with the base case, is selected for further investigations on the other two reactive power support functions, i.e. constant *PF* and constant *Q* control. As the PV penetration level increases, only the capacities of the residential PV systems, including both the existing ones and the newly deployed ones, increase while the capacities of the medium and large PV power plants maintain the same.

The load flow simulation results are presented by the average values over one complete year (8760 data points). The power loss of the complete MV grid at different PV penetration levels is plotted in Figure 1.5-11, with the x-axis representing the ratio of actual installation capacity and 100 MW, (i.e. penetration level of 100%, the representation is the same for the rest figures in this case). The loss first decreases and then increases as the penetration level varies from the base case (22%) to 100%.
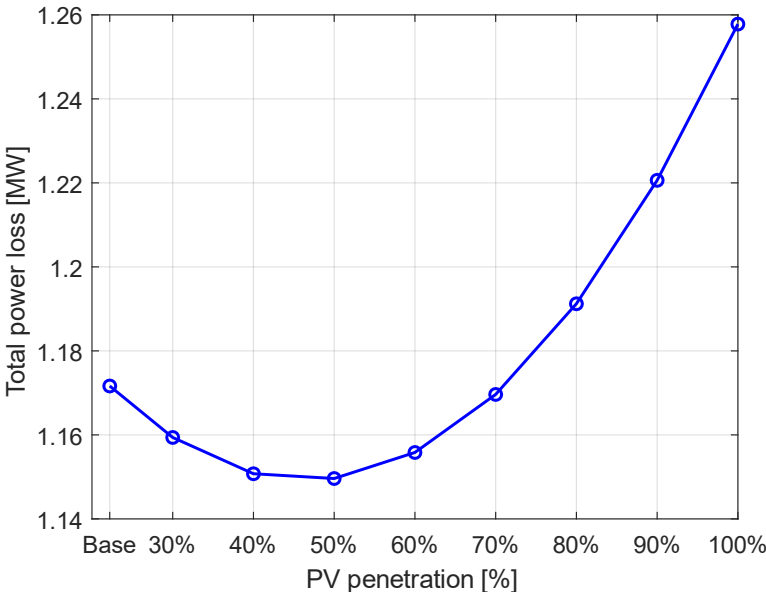

Figure 1.5-11 Total power loss of the entire system at different penetration levels (With *PF*(*P*) control implemented)

The assessment of system power loss takes the loss of the low voltage (LV) feeders into consideration as well. With a generic LV network consisting of 32 buses connected to a 100 kVA transformer, the power loss of the rest LV feeders can be evaluated by scaling up and down the loss of the 100 kVA feeder by the ratio of the actual transformer capacities divided by the 100 kVA. The power loss of the LV feeder connected to a 200 kVA transformer, for example, is the power loss of the 100 kV feeder multiplied by 2 and the rule is the same for the other LV feeders.

According to the values in Figure 1.5-11, it can be observed that the power loss of the whole MV system is around 5% of the load (approximately 23.5 MW on average), which is an acceptable level. The power loss reaches its minimum when the penetration level comes to 40% to 50%. It is seen that the increasing integration of PV systems in the grid contributes to reducing the power loss to some extent. This is because the increase in PV penetration results in higher self-consumption level at the loads, which means that the load demand can be partly or sometimes even completely covered by the PV generation. The active power injected into the buses is therefore reduced.

The over-voltage situations of the buses, including the average hours of buses experiencing over-voltage, the maximal number of buses with the over-voltage problem and the maximal voltage among all the buses, are plotted in Figure 1.5-12a, b and c, respectively. The results in Figure 1.5-12b and c indicate the most severe over-voltage situation

It is found that the over-voltage problem in the 0.4 kV buses becomes more and more severe as the penetration level increases as expected, complying with the laboratory test results stated in Section 1.5.2, that active power output of PV inverter can cause voltage rise at the terminals. At the same time, it is seen that although the maximal voltage of 10 kV and 60 kV buses increases as penetration increases, there is no over-voltage problem occurring to them. The over-voltage problems mainly take place on the 0.4 kV buses.


(a) Average hours of bus over-voltage   (b) Maximal number of over-voltage buses
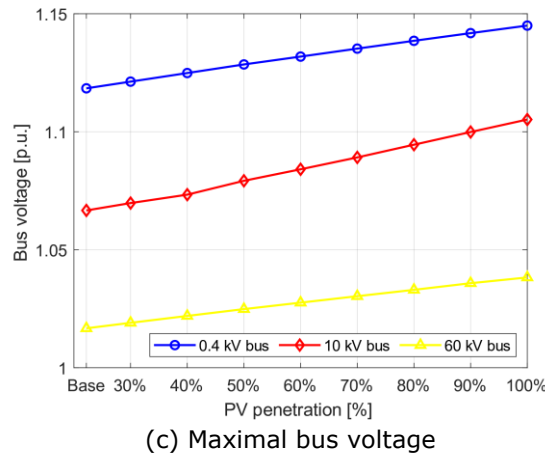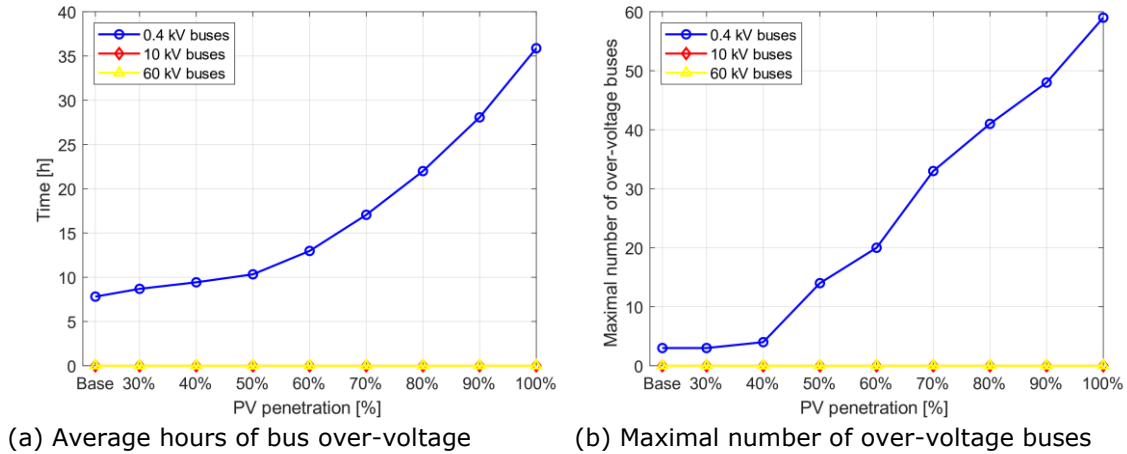
(c) Maximal bus voltage

Figure 1.5-12 Over-voltage situations of buses at different penetration levels (With *PF*(*P*) control implemented)

By comparing the load profile and the PV generation profile, it can be found that the over-voltage problem usually takes place when the PV generation is high and the load demand is low.

The overloading situations of all the transformers within the system (including both the 60/10 kV ones and the 10/0.4 kV ones), including the average hours of being overloaded, the maximal number of overloaded transformers and the maximal loading rate among all transformers, are shown in Figure 1.5-13a, b and c, respectively. The results presented in Figure 1.5-13b and c reflect the most severe overloading situation.

The changing trend of the transformer overloading hours is similar to that of the system power loss and the minimum is reached when the penetration level comes to 40%. To some extent, the increasing integration of PV systems can help lower the stress on the transformers and congestion with the similar reason to the decreasing power loss.
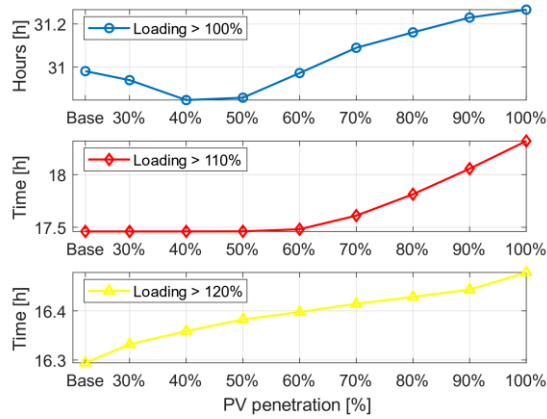
(a) Average hours of all transformers overloading
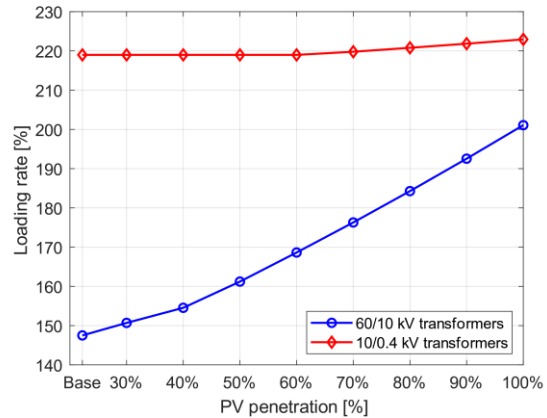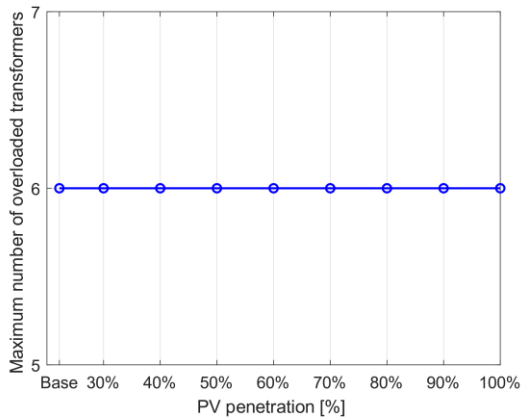
(b) Maximal number of all overloaded transformers

(c) Maximal loading rate

Figure 1.5-13 Overloading situations of transformers at different penetration levels (With *PF*(*P*) control implemented)

From Figure 1.5-13a and b, it is seen that the time of transformers experiencing overload varies as the penetration level increases although the maximal number of the overloaded transformers remains the same during this process. Based on Figure 1.5-13c, it is seen that even though the time of overloading drops with the penetration between 22% and 40%, the highest loading rate of the transformers increases. By checking the load profile and the PV generation profile, it can be found that the transformers can work with overloading problem when the PV generation is high and load demand is low where much power surplus needs exported, or when the PV generation is low and the load demand is high where much power needs to be imported to meet the demand.

According to the results in Figure 1.5-13a, it can be observed that the hours of transformer loading over 100% are at their lowest at 40% penetration. Besides, as shown in Figure 1.5-13c, the maximal loading rate increases faster when the penetration level is above 40%. Based on these results, the penetration level for further studies on other reactive power support functions, i.e. constant *PF* control and constant *Q* control, is selected to be 40%. Then the constant *PF* control is investigated with the base case and the 40%-penetration case. The range of the power factor setpoint is between 0.8 inductive and 0.8 capacitive, with a step of 0.1. Totally 5 cases are compared in this part. The total power loss of the system is plotted in Figure 1.5-14, with the x-axis representing the power factor (the representation is the same for the rest figures in this case).

By comparing the 40%-penetration case with the base case, likewise, it is found that certain penetration level of PV systems in the grid contributes to the reduction in the power loss of the system. Additionally, compared with the previous case where the *PF*(*P*) control is implemented, the system power loss is slightly higher. Besides, it is also observed that the power loss in the base is lower than the 40%-penetration case when the power factor is smaller

than 0.9 (inductive) and then larger when the power factor increases to unity and then to capacitive.
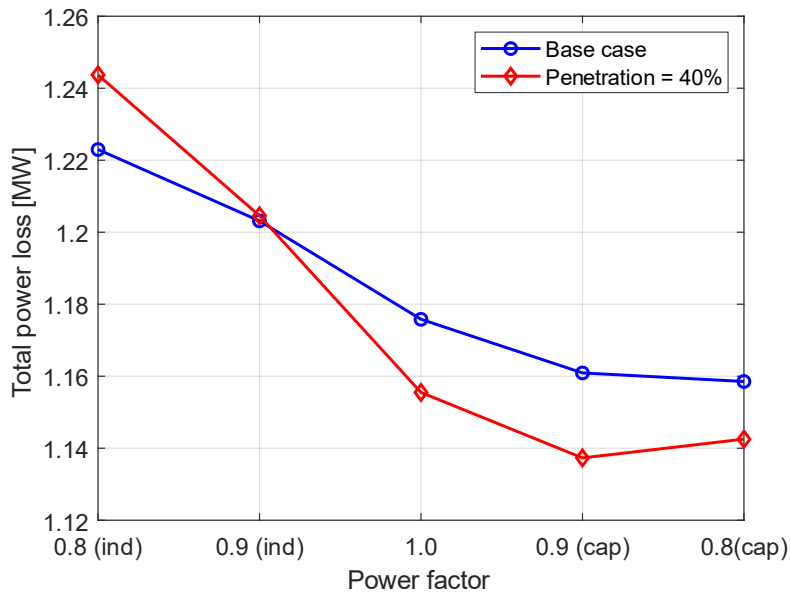

Figure 1.5-14 Total power loss of the entire system with different *PF* values (With constant *PF* control implemented)

Additionally, from Figure 1.5-14, it is found that the loss decreases as the power factor approaches unity and starts increasing when the power factor becomes "more capacitive". Capacitive reactive power means that the inverters absorb reactive power instead of generating. The decrease in the power loss as the power factor becomes capacitive is potentially related to the cables. Because the cables, different from the overhead lines which are usually modelled as inductive elements, are more capacitive.

The over-voltage situations of the buses are plotted in Figure 1.5-15. The results in Figure 1.5-15b and c indicate the most severe over-voltage situation in this case. By comparing the results plotted in Figure 1.5-12 and 1.5-15, it can be found that the over-voltage problem, in this case, is worse than the case with the *PF*(*P*) control implemented. It, in general, has more buses with the over-voltage problem and higher maximal bus voltage magnitude. However, it can also be found that the over-voltage problem gets improved as the power factor goes towards capacitive. Because the cables are capacitive, they usually have a voltage rise at the receiving end of the line, and this can explain the decreasing in the over-voltage time and the maximal voltage at the buses.
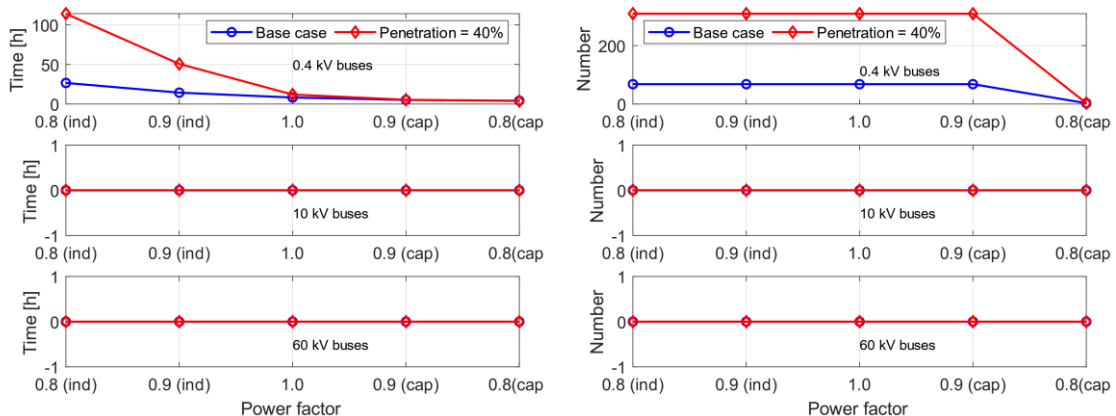

(a) Average hours of bus over-voltage

(b) Maximal number of over-voltage buses
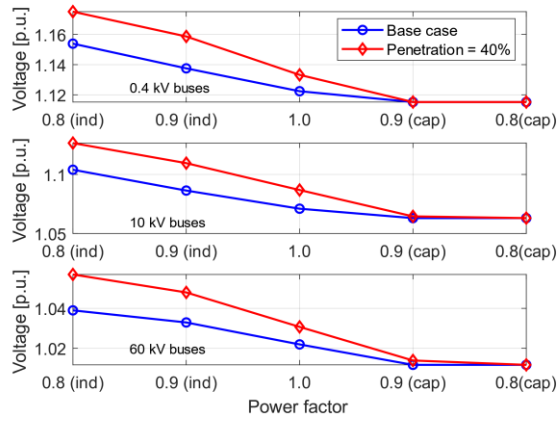
(c) Maximal bus voltage

Figure 1.5-15 Over-voltage situations of buses in the system with different power factor set points (With constant *PF* control implemented)

The overloading situations of the transformers (including both the 60/10 kV ones and the 10/0.4 kV ones) are plotted in 1.5-16. The results in Figure 1.5-16b and c indicate the most severe overloading situations. According to the results, there are only 2 to 3 transformers that reach such high loading rate (over 200%). Similar results can be seen in the next case (with constant *Q* control applied).
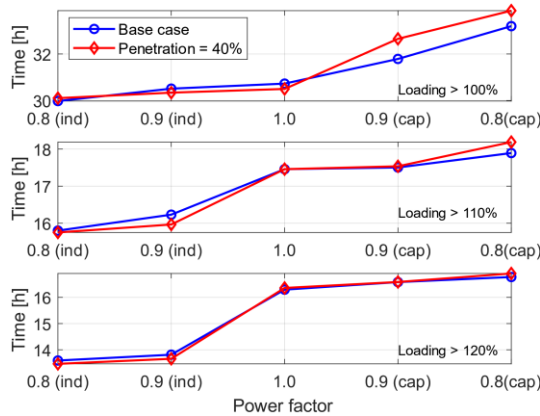
(a) Average hours of transformers overloading
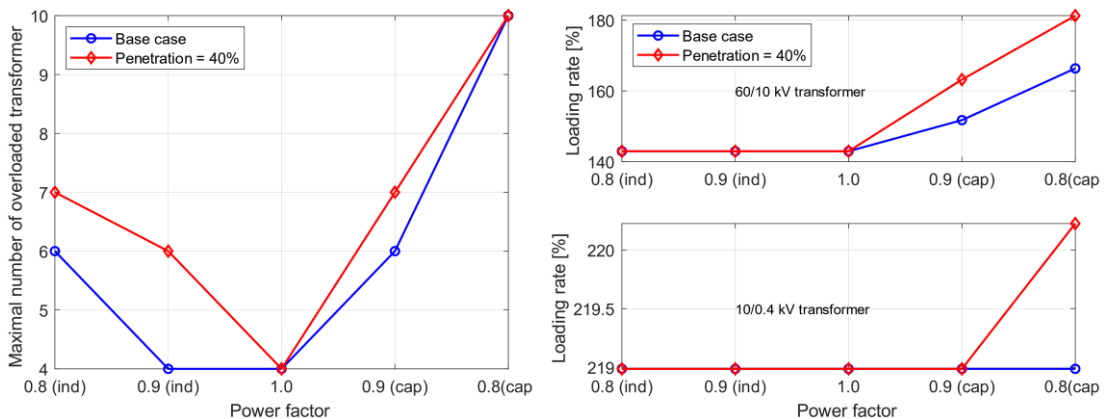
(b) Maximal number of overloaded transformers

(c) Maximal loading rate

Figure 1.5-16 Overloading situations of transformers with different power factor set points (With constant *PF* control implemented)

Based on the comparison between the results in Figure 1.5-13 and 1.5-16, it is observed that the overloading problems in the transformers in this case and the case with *PF*(*P*) control implemented are quite close to each other. The maximal number of overloaded transformers, in this case, reaches its lowest value with unity power factor. Additionally, the maximal loading

rate of the 60/10 kV transformers increases more rapidly when the power factor moves to capacitive from unity.

Similarly, in this case, the over-voltage problems in the buses mostly occur when the PV generation is high and load demand is low, while the overloading problems in the transformers in the system mostly happen in the condition of high PV generation and low load demand or low PV generation and high load demand.

As stated previously, because the constant Q control is only applied to medium- and large-scale PV power plants rather than residential PV systems in the real world, in the case where the constant Q control function is investigated, the control strategies of the residential PV systems in the LV level should either be $PF(P)$ or constant PF. Furthermore, by comparing the results on power loss presented in Figure 1.5-11 and 1.5-14, the system power loss is lower with the constant PF control implemented.

From Figure 1.5-14, it can be observed that the lowest power loss appears when the power factor is equal to 0.9 (capacitive). However, according to TF 3.2.1 and TF 3.2.2, the set point of constant power control lies in the over-excited area [4], [5], namely inverter generating both active and reactive power. Furthermore, the number of overloaded transformers increases faster when the power factor becomes capacitive. Therefore, in this case, the control function for all the residential PV systems is selected to be the constant PF control with the set point being a unity power factor.

According to the relation between active power P, reactive power Q and apparent power S, i.e. $S = \sqrt{P^2 + Q^2}$, the theoretical value of the maximum reactive power that can be provided by a generation unit is $\frac{S}{\sqrt{2}}$, equivalent to approximately 70% of its apparent power. Identical to the requirements on the constant PF control, according to TF 3.2.1 and TF 3.2.2, the set point of reactive power for the constant Q control also lies within the over-excited zone [4], [5]. Therefore, only positive set points, namely inverters generating reactive power instead of absorbing, are considered in this case, including 10%, 30%, 50% and 70% of the apparent power of the PV inverter, 4 cases in total to be studied and compared.

The power loss of the entire system, in this case, is presented in Figure 1.5-17, with the x-axis representing the ratio of reactive power set point and the installed capacity of the PV inverter (i.e. Q/S, the representation is the same for the rest figures in this case).
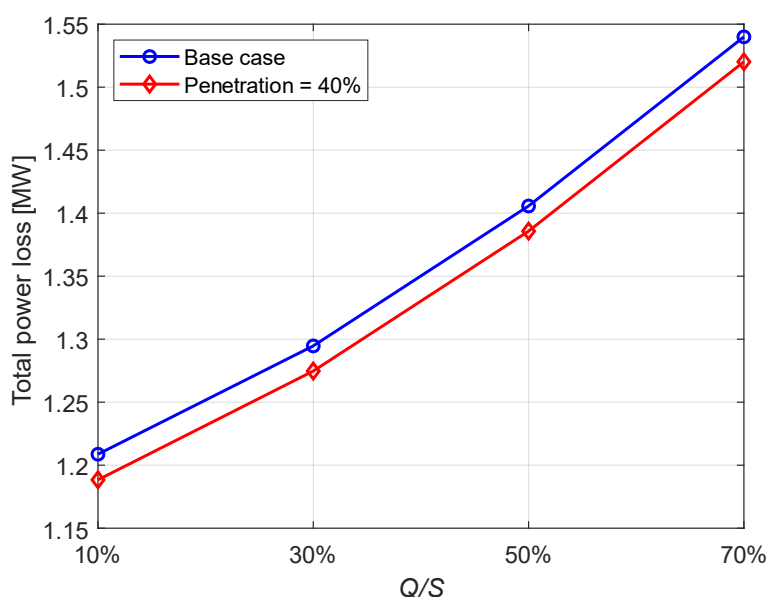

Figure 1.5-17 Total power loss of the entire system with different Q set points (With constant Q control implemented)

By comparing the results on the system power loss in Figure 1.5-17, 1.5-11 and 1.5-14, it can be found that the system power loss in this case, which is equivalent to 6% to 7% of the average load, is higher than the other two cases with the *PF(P)* control and the constant *PF* control implemented. Furthermore, the power loss increases as the reactive power set point increases.

The over-voltage situations of the buses are presented in Figure 1.5-18. Among the three figures, the results in b and c reflect the most severe over-voltage situation. With the set point of the reactive power increases, the over-voltage problem becomes more and more severe as expected. The time of buses experiencing over-voltage and the number of buses with the problem increase. Because the need of reactive power can vary during the system operation, the reactive power provided by the inverters can be higher than the need of the system, which causes voltage rise problems at buses and this can also cause extra power losses in the system as indicated in Figure 1.5-17. Moreover, as the experiment results discussed in Section 1.5.2, where the inverter outputs reactive power trying to regulate the voltage upwards when there is an under-voltage problem, the output of reactive power when no under-voltage problem can cause an over-voltage problem. With the PV penetration level increases, the over-voltage problem potentially becomes worse according to the comparison between the base case and the 40%-penetration case in Figure 1.5-18.
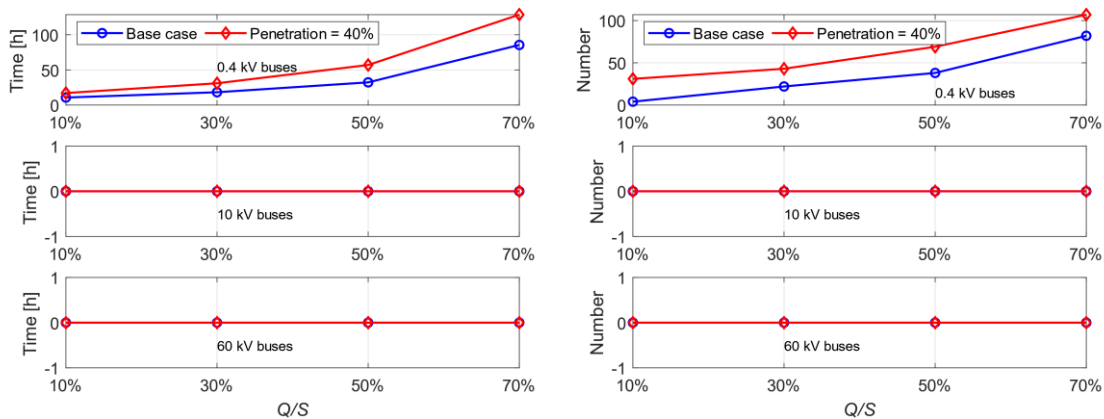
(a) Average hours of bus over-voltage (b) Maximal number of over-voltage buses
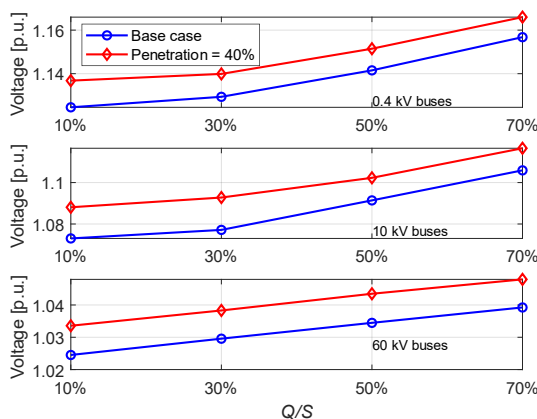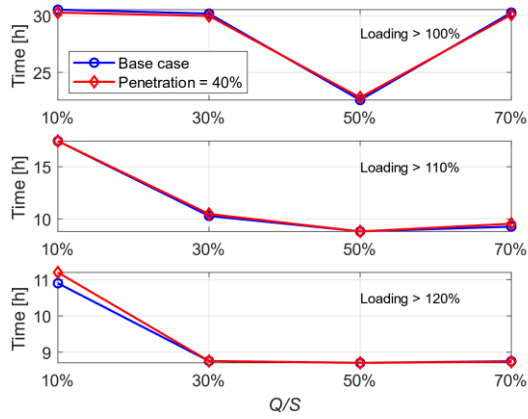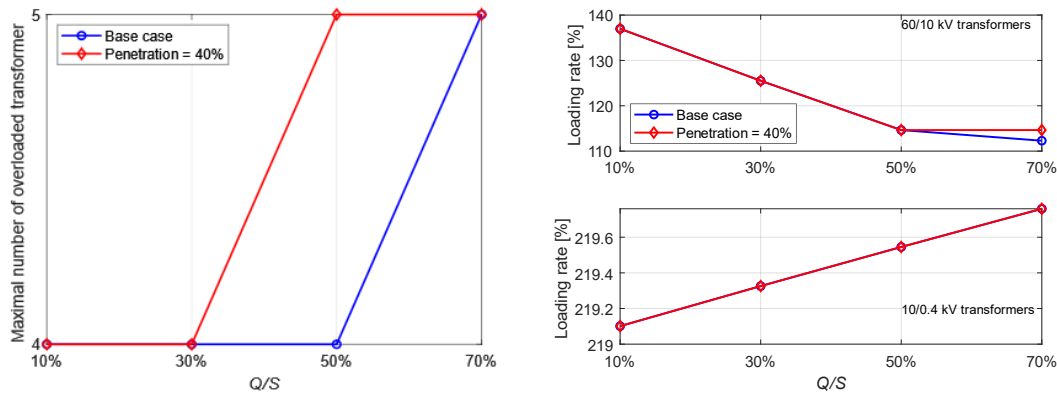

(c) Maximal bus voltage

Figure 1.5-18 Over-voltage situations of buses in the system with different *Q* set points (With constant *Q* control implemented)

The overloading situations of the transformers (including both the 60/10 kV ones and the 10/0.4 kV ones) are presented in Figure 1.5-19. The results in Figure 1.5-16b and c indicate the most severe overloading situation in this case.

(a) Average hours of all transformers overloading

(b) Maximal number of overloaded transformers

(c) Maximal loading rate

Figure 1.5-19 Overloading situations of transformers with different Q set points (With constant Q control implemented)

Generally, it can be seen that the situation is close to the previous two cases. However, it is found that when the reactive power set point is 50% of the inverter capacity, the overloading hour reaches its minimum and the maximal loading rate of 60/10-kV transformers decreases while that of the 10/0.4-kV transformers increases. Because there is a need for reactive power in this power system as mentioned above, the reactive power is transmitted through the transmission lines and distribution transformers, potentially causing overloading. Therefore, the increasing reactive power support from the PV systems can relieve the stress. This can be the reason for the decreasing overloading time of the transformers and the maximal loading rate of the 60-10 kV transformers. However, at the same time, the increasing reactive power can worsen the overloading problem in the 0.4/10-kV transformers, as indicated in the lower plot in Figure 1.5-19c.

The over-voltage problems in the buses and the overloading problems in the transformers in the system mostly take place for the same reason as the previous two cases, namely the big mismatch between the PV generation and the load demand.

1.6   Utilization of project results

The DSO at Bornholm has experienced an increased need for compensating the capacitive issue (overvoltage) due to digging down cables replacing overhead lines. Taking advantage of decentralized resources in the grid, have been embraced because in this project because it can pave the way for further utilization of e.g. ancillary services from larger PV plants – delivering reactive power also at night. The PVTP project began long before the 2 x 7,5 MW PV plants were even known by the DSO, but due to the PVTP project, much of the practical solutions communicating with a PV plant could be replicated seamless. The SCADA screen for the test site was expanded with two columns for the new PV plants.
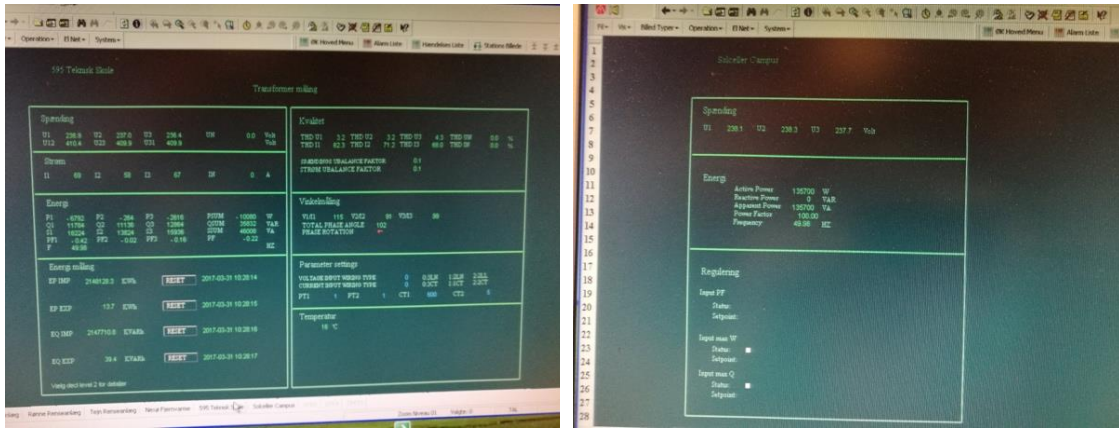
Photo 3. Screenshot of the implemented measurement and control system in the control room at BOEF.

Inspired by BEOF plant, the new PV plant constructed at DTU by DTU Campus Service has adopted the same protocol for the inverters. This means the inverters will comply with Sunspec protocol for communication. The experience from PVTP has inspired the newly installed PV plants in DK.

Journals, conferences, reports and press releases	**Status**
[1]. ZY Wang, Guangya Yang, "Impact of solar PV on the medium voltage network in distribution grids", Energies, vol 12, no. 8, 2019. Doi:https://doi.org/10.3390/en12081458	To be submitted
[2]. ZY Wang, T.B. Rasmussen, Guangya Yang, "Test of PV inverters under unbalanced operations", invited conference publication to IET Renewable Power Generation with an extension.	To be submitted
[3]. ZY Wang, T.B. Rasmussen, Guangya Yang, "Test of PV inverters under unbalanced operations", The 7th International Conference on Renewable Power Generation, DTU, Lyngby, Copenhagen, Denmark, 26 - 27 September 2018.	Published
[4]. G.Y. Yang, J.K. Zimmermann, H.H. Ipsen, T.V. Hansen, K.H.B. Frederiksen, S.B. Kjær, T. Helth, "Solar Inverters as a part of DSO grid control functions", The 7th International Conference on Renewable Power Generation, DTU, Lyngby, Copenhagen, Denmark, 26 - 27 September 2018.	Published
[5]. EU PV Technology Platform, white paper on "Assessing the need for better forecasting and observability of PV", published. Online. Available: http://www.etip-pv.eu/publications/etip-pv-reports.html	Published
[6]. EU PV Technology Platform, inverter review paper on "The inverter as multi-purpose control element: a review", in draft, to be submitted to Solar Energy.	Draft
[7]. The project result has been used in several reports which have been published by the IEA PVPS Task 14 working group focussing on High Penetration of PV Systems in Electricity Grids.	
[8]. Danish Energy article ended up being one of summer's most read article. Available: https://lnkd.in/gew7wdk.	Published
[9]. The article was shared by other media like Finans.dk, LinkedIn, Facebook, Energywatch etc. At LinkedIn + 6,100 views and at danskenergi.dk + 1,000. Unique views were registered, indicating great interest in our project.	

Student projects offered

[1]. Operation and control of solar PV plant in the LV network, 1 Oct 2016 – 15 Feb 2016.	Finished
[2]. Studies on PV inverter under unbalanced operation, 1 Sep 2017 – 31 Dec 2017	Finished

Courses with related learning activities

[1]. PV tutorial for short training on PV technology and grid connection issues.   Finished

1.7   Project conclusion and perspective

The project has clearly shown that it is possible to connect the utility control system to solar plant and control them according to the grid rules. This experience has been disseminated to other DSO's and utility-scale PV plant owners. We have seen that we are able to run the solar inverters from the control room and also control them during the night time. In this way, the grid can benefit from voltage control and reactive power generation when needed. This can be a cheaper solution for BEOF than purchasing the reactive power via the sea cable from Sweden. For the PV owner, there could be a potential income by offering these kinds of ancillary services.

Measures had to be taken to protect the utility fibre communication system against unwished access, so direct access to the inverter system was not possible because this inverter is connected to the Internet via the local network at the Campus plant (Bornholm). Therefore an RTU (remote terminal unit) was installed to secure a physical firewall and communication interface. This brings extra cost into the control system and will be a barrier to utilize the possibility of controlling smaller PV plants in the grid. Smaller PV systems will have to run by static control functions as stated in Teknisk Foreskrift 3.2.1.

The partners have seen a potential market for a low-cost RTU which easily can be installed and controlled by the utility in medium size PV plants.

In the second part, experiments are performed on a PV inverter system to investigate its performance under unbalanced operation and fault conditions. Because of the increasing penetration of PV systems at the low voltage networks which usually operate in an unbalanced condition, the results are beneficial for further study on protection and integration.

During unbalanced operations, with $Q(V)$ control applied, the PV inverter reacts to the under- and over-voltage situations by generating and absorbing reactive power. The amount of the reactive power is controlled by the positive sequence voltage and proportional to that under the balanced operation. The active power output maintains constant, indicating that the control strategy of the inverter is to guarantee the active power production. With the $PF(P)$ control applied, the power factor maintains constant due to the constant active power. By comparing all three scenarios, the frequency response function is affected by the unbalanced operation regarding the activation of the support. The function responds slower under the unbalanced conditions. This is likely caused by the change in reference active power caused by the change in positive sequence voltage. Although there are effects on the function, the activation point is still in compliance with Teknisk Foreskrift 3.2.1.

During all three fault conditions, the inverter contributes fault current into the grid which can enable the protection schemes to detect the fault and trip the circuit breakers to clear it. The fault current is the highest in balanced fault while the lowest in double-phase fault, and the fault current is regardless the actual active power output but affected by the full capacity of the inverter. The fault current affects the disconnection time of the inverter. Higher fault current leads to shorter disconnection time.

In the third part, three cases are studied on the distribution grid on Bornholm at the medium voltage level, where three different reactive power support functions of PV systems, including $PF(P)$, constant PF and constant Q control, are investigated at different penetration level in terms of their impacts on the entire system, including power loss of the entire system, overloading of transformers and over-voltage problem of the buses within the system.

With $PF(P)$ control implemented, different penetration levels are investigated. It is found that the system power loss first decreases and then increases as the penetration level increases from the base case (22%, 22 MW) to 100% (100 MW). At the penetration level of 40%, the power loss of the entire system and the time of the transformers experiencing overloading

problem reach their minimum. Generally, the overloading situation of the transformers and the over-voltage in the buses become more and more severe as the penetration level increases as expected. Overloading mostly happens when the demand is high and the PV generation is low or when the demand is low and the PV generation is high. The over-voltage problem takes place when the demand is low and PV generation is high.

Based on this, the assessment of the constant *PF* and constant *Q* control is performed at the penetration level of 40% and the base case. Different set points of the power factor and reactive power are tested.

With the constant *PF* control applied, the power loss of the entire system is fairly close to the loss with the *PF*(*P*) control applied, and the power loss is at its lowest when the power factor is 0.9 (capacitive) which is potentially due to the compensation to the capacitive reactive power of the cables in the grid. The overloading problem of the transformers, in this case, is close to that of the case with *PF*(*P*) while the over-voltage problem of the buses is worse in this case. The more severe over-voltage problem, in this case, can be caused by the "surplus" in the reactive power.

With the constant *Q* control implemented in the PV plants (capacity larger than 6 kW), the power loss of the entire system is the highest among all the cases. In general, the overloading problem of the transformers is close to those of the previous two cases. The over-voltage becomes more and more severe as the set point of reactive power increases because the reactive power output from the PV system can be higher than de demand from the system components. However, to some extent, with the reactive power set point at a certain level, the over-voltage problem can get improved.

Based on all three case studies, it is found that the system power loss, the stress put on the transformers and lines can be improved with a certain penetration level of PV systems and different reactive power support functions can affect the system operation.

References

[1] P.-J. Alet *et al.*, "Quantification, challenges and outlook of PV integration in the power system: a review by the European PV Technology Platform," in *31st European Photovoltaic Solar Energy Conference and Exhibition (EU PVSEC)*, 2015, pp. 2945–2951.

[2] P.-J. Alet *et al.*, "Photovoltaics merging with the active integrated grid Grid integration: White paper of the EU PV technology platform, working group on grid integration.," 2015.

[3] SunSpecAlliance, "SunSpec Alliance: Information Standards for Distributed Energy," San Jose, CA, USA, 2015.

[4] Energinet, "Technical Regulation 3.2.1 For Power Plants Up To and Including 11 kW (Plant Category A1)," Energinet, Fredericia, Denmark, Doc. no. 15/01353-94, 2016.

[5] Energinet, "Technical Regulation 3.2.2 for PV Power Plants Above 11 kW," Fredericia, Denmark, Doc. no. 14/17997-39, 2016.

[6] CIGRE, "Benchmark Systems for Network Integration of Renewable and Distributed Energy Resources Task Force C6.04," Paris, France, 2014.

[7] G. B. Andresen, R. A. Rodriguez, S. Becker, and M. Greiner, "The potential for arbitrage of wind and solar surplus power in Denmark," *Energy*, vol. 76, pp. 49–58, 2014.